Nanoscale Res Lett (2007) 2:265–281
DOI 10.1007/s11671-007-9061-9

NANO REVIEW

Are quantum dots ready for in vivo imaging in human subjects?

Weibo Cai · Andrew R. Hsu · Zi-Bo Li · Xiaoyuan Chen

Received: 14 April 2007 / Accepted: 24 April 2007 / Published online: 30 May 2007

Abstract Nanotechnology has the potential to profoundly transform the nature of cancer diagnosis and cancer patient management in the future. Over the past decade, quantum dots (QDs) have become one of the fastest growing areas of research in nanotechnology. QDs are fluorescent semiconductor nanoparticles suitable for multiplexed in vitro and in vivo imaging. Numerous studies on QDs have resulted in major advancements in QD surface modification, coating, biocompatibility, sensitivity, multiplexing, targeting specificity, as well as important findings regarding toxicity and applicability. For in vitro applications, QDs can be used in place of traditional organic fluorescent dyes in virtually any system, outperforming organic dyes in the majority of cases. In vivo targeted tumor imaging with biocompatible QDs has recently become possible in mouse models. With new advances in QD technology such as bioluminescence resonance energy transfer, synthesis of smaller size non-Cd based QDs, improved surface coating and conjugation, and multifunctional probes for multimodality imaging, it is likely that human applications of QDs will soon be possible in a clinical setting.

Keywords Quantum dot (QD) · Nanoparticles · Nanotechnology · Cancer · Molecular imaging · Near-infrared fluorescence (NIRF) imaging · Nanomedicine

W. Cai · A. R. Hsu · Z.-B. Li · X. Chen (✉)
The Molecular Imaging Program at Stanford (MIPS), Department of Radiology and Bio-X Program, Stanford University School of Medicine, 1201 Welch Rd, P095, Stanford, CA 94305-5484, USA
e-mail: shawchen@stanford.edu

Introduction

To expedite the clinical application of nanotechnology, the National Cancer Institute (NCI) is currently funding eight Centers of Cancer Nanotechnology Excellence (CCNEs) and twelve Cancer Nanotechnology Platform Partnerships (http://nano.cancer.gov/). It is believed that combining development efforts in nanotechnology and cancer research may quickly and effectively transform the prevention, diagnosis, and treatment of cancer in the future. After establishing an interdisciplinary nanotechnology workforce, the goal was to have matured nanotechnology into a clinically useful field by 2010. The NCI Alliance for Nanotechnology in Cancer aims to develop research tools to help identify new biological targets, agents to monitor predictive molecular changes and prevent precancerous cells from becoming malignant, imaging agents and diagnostics to detect cancer in the earliest pre-symptomatic stage, multifunctional targeted devices to deliver multiple therapeutic agents directly to the tumor, systems to provide real-time assessment of therapeutic and surgical efficacy, and novel methods to manage symptoms that reduce the quality of life. The nanoparticles actively being pursued include quantum dots (QDs) [1, 2], nanotubes [3], nanowires [4], nanoshells [5], and many others [6–9]. Among these, QDs are the most widely studied and have many potential clinical applications.

Organic fluorophores and dyes have been historically used to label cells and tissues for both in vitro and in vivo imaging [10]. However, due to their inherent photophysical properties such as low photobleaching thresholds, broad absorption/emission spectra, and small Stokes shifts, their use is limited and they are not ideal agents for multiplexing, long-term, or real-time imaging. On the other hand, QDs are inorganic fluorescent semiconductor nanoparticles

with superior optical properties compared with organic fluorophores [11, 12]. QDs have unique size- and composition-dependent optical and electrical properties due to quantum confinement, hence their commonly used name of quantum dots [13, 14]. QDs have many desirable properties for biological imaging, such as high quantum yields, high molar extinction coefficients (1–2 orders of magnitude higher than organic dyes), strong resistance to photobleaching and chemical degradation, continuous absorption spectra spanning UV to near-infrared (NIR; 700–900 nm), long fluorescence lifetimes (>10 ns), narrow emission spectra (typically 20–30 nm full width at half maximum), and large effective Stokes shifts [15–22]. Excitation-emission matrix analysis has shown that QDs always emit the same wavelength of light no matter what excitation wavelength is used [23]. Therefore, multiple QDs with different emission spectra can be simultaneously visualized using a single excitation source (Fig. 1). Since the emission spectrum of each QD is narrow, the fluorescence signal of each QD can be readily separated and individually analyzed based on the emission spectrum in order to achieve multiplexed imaging.

QDs and their advantageous photophysical properties have given researchers new opportunities to explore advanced imaging techniques such as single molecule or lifetime imaging while also providing new tools to revisit traditional fluorescence imaging methodologies and extract previously unobserved or inaccessible information. Given their ability to cover nano, micro, and macro length scales, QDs are particularly useful to study the wide range of diverse molecular and cellular events involved in the pathology of diseases such as cancer. Since the first demonstration of the biomedical potential of QDs in 1998 [1, 2], QD-based research has increased exponentially in recent years. In less than a decade, QDs have overcome many of the intrinsic limitations of traditional fluorophores and become powerful tools in fields such as molecular biology, cell biology, molecular imaging, and medical diagnostics. The purpose of this review is to summarize and highlight the biomedical applications of QDs to date and address future research directions, obstacles, and potential uses of QDs for clinical applications.

QD synthesis and conjugation strategies

QDs made directly in water often have a wide range of size distributions while QDs synthesized at high temperature (300 °C) in organic solvents are more monodisperse [21, 24–26]. Surface passivation by depositing an inorganic capping layer (or shell) composed of a semiconductor material with a wider band gap than the core material can significantly increase the quantum yield, protect it from oxidation, and prevent leaching of Cd or Se into the surrounding solution [21, 27, 28]. Over the past decade, a variety of procedures have been developed for synthesizing high quality QDs, all of which are based on the initially reported high-temperature pyrolytic reaction [25]. QDs used in biomedical applications are colloidal nanocrystals typically synthesized from periodic groups of II–VI (e.g. CdSe, CdTe) or III–V (e.g. InP, InAs) including two- and three-element systems [25–31]. Depending on the component and size of the core, the emission peak can vary from UV to NIR wavelengths (400–1350 nm). Over the years, QD synthesis has become relatively simple, inexpensive, and highly reproducible with minor complications.

QDs synthesized in organic solvents typically have hydrophobic surface ligands [20, 21]. In order to make them water soluble, surface functionalization with hydrophic ligands can be achieved in many ways [21, 32]. For a comprehensive review, the readers are referred to ref. [21]. The first technique involves ligand exchange. The native hydrophobic ligands are replaced by bifunctional ligands which contain surface anchoring moieties (e.g. thiol) to bind to the QD surface and hydrophilic end groups (e.g. hydroxyl and carboxyl) to render water solubility [2, 33]. The second strategy employs polymerized silica shells functionalized with polar groups to insulate the hydrophobic QDs [1]. While nearly all carboxy-terminated ligands limit QD dispersion to basic pHs [34], silica shell

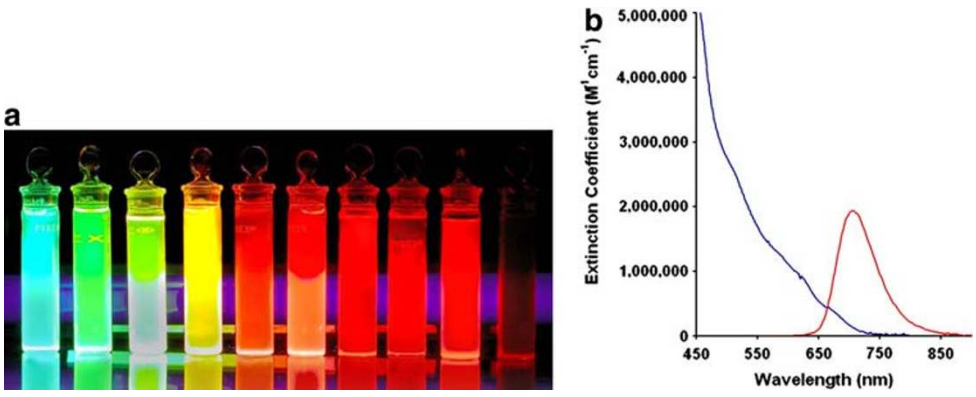

Fig. 1 (**a**) A series of QDs of different core size and emission wavelength can be excited simultaneously by a single excitation light source. (**b**) Representative excitation (blue) and emission (red) spectra of QDs.

encapsulation provides stability over a much broader pH range [35]. The third method maintains the native ligands on the QDs and uses variants of amphiphilic diblock and triblock copolymers and phospholipids to tightly interleave the alkylphosphine ligands through hydrophobic interactions [36–38]. Aside from rendering water solubility, these surface ligands serve a critical role in insulating, passivating, and protecting the QD surface from deterioration in biological media.

Water soluble QDs can be functionalized through a diverse array of conjugation strategies due to the large surface area to volume ratio of QDs which provides numerous surface attachment points for functional groups. First, carboxylic acid groups on the QD surface can react with amines via EDC coupling [39, 40]. This strategy has been widely used to produce QD-streptavidin conjugates which can then be used to attach biotinylated molecules [41, 42]. The versatility of QD-streptavidin conjugates makes them attractive bioprobes, but the additive volume of QDs, streptavidin, and extra layer(s) of functional molecules limits their potential applications. The immunogenecity of streptavidin is also a concern for applications in living subjects [43]. EDC coupling can sometimes give intermediates which easily aggregate and can also make it difficult to control the number of molecules attached to the surface of a single QD. In an attempt to reduce the overall size of the QD conjugate, researchers have used direct cross-linking to attach ligands to the QD surface [44]. Second, the amine groups on the QD surface can react with active esters or they can be converted to maleimide (through a heterobifunctional cross-linker) for Michael addition of a sulfhydryl group in thiolated peptides, cysteine-tagged proteins, or partially reduced antibodies [45]. Third, the hydrophobic coating of QDs can be replaced with thiolated peptides (to form thiol-bonding between sulfhydryl groups and sulphur atoms on the QD surface) or polyhistidine-containing proteins (histidine residues can coordinate to the QD surface Zn atoms via metal complexation) thus enabling direct attachment of proteins/peptides to the QD surface [46–50]. Finally, QD conjugation can also be achieved via adsorption or non-covalent self-assembly using engineered proteins [51–54].

Research has shown that a three-layer method using an antibody against a specific target, a biotinylated secondary antibody against the primary antibody, and a streptavidin coated QD can effectively label target molecules with QDs [38, 42]. This strategy is not limited to antibodies. QD-streptavidin conjugates are commercially available and can be used to attach virtually any biotinylated molecule to a QD surface. Although the overall size of the resulting QD conjugates are relatively large (>20 nm), this is not a major concern for in vitro applications. Two of the most prominent problems in QD functionalization are the lack of homogeneity when attaching surface proteins to QDs and the difficulty in precisely controlling the protein-to-QD ratios. Both of these complications may result in QD conjugates with misaligned protein orientations or large aggregates of surface proteins which are not fully functional or potentially nonfunctional. Although the biological function of these molecules has not been severely affected by QD conjugation in most reports, advances in conjugation strategy/chemistry are still needed in the future to provide a robust platform for QD functionalization.

QDs for in vitro and cell-based applications

Numerous in vitro and cell-based uses have been discovered for QDs because of their unique photophysical properties [22, 55–58]. QDs can be used in place of traditional organic dyes in virtually any system and outperform dyes in the majority of cases. The major advantage of QDs is their strong resistance to photobleaching over long periods of time (minutes to hours), allowing acquisition of images with good contrast and signal intensity. Most QDs are much brighter than organic dyes due to the combination of higher extinction coefficients ($0.5–5 \times 10^6$ M^{-1} cm^{-1}) and higher quantum yields [20, 21]. QDs have been used in a vast number of in vitro and cell-based applications.

Cellular labeling

In recent years, QDs have made the most progress and drawn the greatest interest in the area of cellular labeling. Numerous cellular components and proteins (in live or fixed cells) have been labeled and visualized with functionalized QDs, such as the nuclei, mitochondria, microtubules, actin filaments, cytokeratin, endocytic compartments, mortalin, and chaperonin proteins [51, 59–62]. The cell membrane proteins and receptors that have been labeled with QDs include prostate specific membrane antigen (PSMA), HER kinases, glycine receptors, serotonin transport proteins, p-glycoprotein, band 3 protein, and many others [20, 21, 37, 38, 42, 44, 63–67]. The excellent photostability of QDs is particularly useful for continuous illumination of three dimensional (3D) optical sectioning using confocal microscopy, where image reconstruction and quality has been severely limited by photobleaching of organic fluorophores [66, 68]. High sensitivity combined with virtually an unlimited number of well-separated colors all excitable by a single light source also makes QDs ideal probes for multiplexed cellular imaging (a representative example is shown in Fig. 2) [21, 68, 69].

One of the most interesting aspects of QDs for use in immunofluorescence techniques is the small number of QDs necessary to generate a detectable signal. A number of

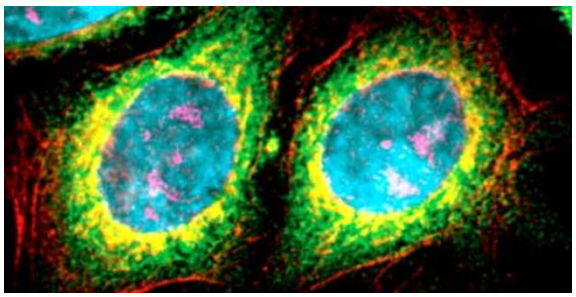

Fig. 2 Pseudocolored fluorescence image depicting five-color QD staining of fixed human epithelial cells. The nucleus, Ki-67 protein, mitochondria, microtubules, actin filaments were each labeled with a QD of different emission wavelength. From [21]

studies have reported QD flickering in cellular specimens, a phenomenon termed ''blinking'' [70, 71]. QD blinking has shown that an individual QD can be observed with a sensitivity limit of one QD per target molecule in immunocytological conditions using current microscopy technology. QD blinking can be overcome by passivating the QD surface with thiol moieties [72] or by using QDs in free suspension [73].

Cell tracking

As a result of their high photostability, QDs can be effectively tracked over an extended period of time in order to monitor cellular dynamics including movement, differentiation, and fate [36, 42, 63, 74]. Large quantities of QDs can be delivered into live cells using a variety of different techniques such as microinjection [36], peptide-induced transport [75], electroporation [76], and phagocytosis [63]. Once internalized, QDs can spread to daughter cells during cell division. Lectin-coated QDs have been used to label gram-positive bacteria and a single QD can be tracked for several minutes as it diffuses into the membrane of live cells and moves within the cytosol [77]. QD-peptide conjugates have been transfected and retained in living cells for up to a week without detectable negative cellular effects [59]. Cellular endocytosis of QDs has also been studied in which the endocytosis efficiency of 15 nm QD conjugated sugar balls was compared with that of 5 nm and 50 nm particles and it was found that endocytosis was highly size dependent [78]. All these cell tracking studies would not have been possible to perform using traditional organic dyes.

Fluorescent in situ hybridization (FISH)

FISH uses fluorescently labeled DNA probes for gene mapping and identification of chromosomal abnormalities [79, 80]. FISH allows for visualization and mapping of cellular genetic material in order to quantify gene copy numbers within tumor cells that have abnormal gene amplification. DNA or oligonucleotides have been conjugated to QDs, and results from in vitro and cell-based assays have shown that these conjugates retain their ability to form complementary sequences of Watson-Crick base pairs [36, 81–88]. The significantly brighter and more photostable fluorescence signals of QD over organic dyes can allow for more stable and quantitative uses of FISH for research and clinical applications (Fig. 3) [81]. It has recently been reported that the fluorescence intensity of QD-streptavidin based FISH probes varied according to the pH of the final incubation buffer [89]. However, the exact mechanism of this varying fluorescence has yet to be clarified. Recently, direct multicolor imaging of multiple subnuclear genetic sequences using QD-based FISH probes was achieved in *Escherichia coli* [90].

Fluorescence resonance energy transfer (FRET)

FRET is a process in which energy is transferred from an excited donor to an acceptor via a resonant, near-field dipole–dipole interaction [91]. FRET is sensitive to the distance between the donor and the acceptor on the 1–10 nm range, a scale correlating to the size of biological macromolecules. FRET has been used with conventional organic dyes and fluorescent proteins in order to monitor intracellular interactions and binding events, but the results have been suboptimal [92, 93]. QDs were first reported for FRET applications in 1996 [94, 95], and since then,

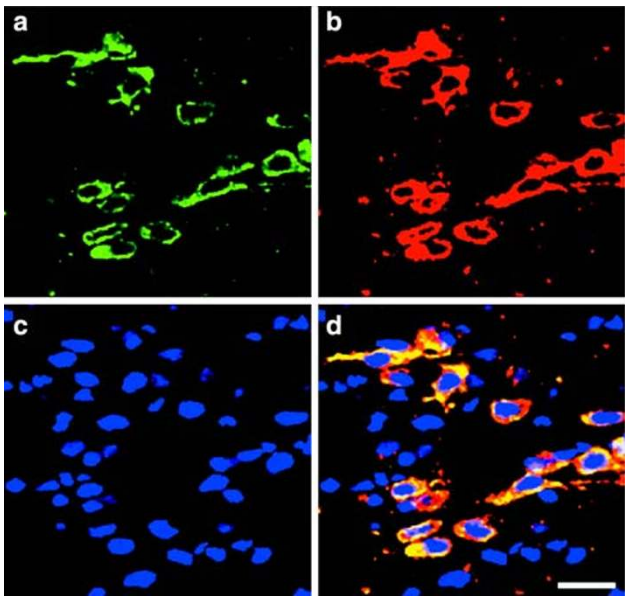

Fig. 3 Double labeling FISH using QD525 and QD585 oligonucleotide probes. The same mRNA was detected with both QD525 (**a**) and QD585 (**b**) probes. DAPI (**c**) staining and overlayed images (**d**) are also shown. Scale bar = 20 μm. From [81]

numerous studies have demonstrated the use of QD-based FRET in biological systems where QDs can be either energy donors or acceptors [48–50, 96–102].

There are two distinct advantages of using QDs as FRET donors over organic fluorophores. First, QD emission can be size-tuned to increase the spectral overlap with a specific acceptor dye. Second, FRET efficiency can be significantly improved when several acceptor dyes interacting with a single QD donor [48]. Using a 6 nm QD with a dye-labeled protein attached to the QD surface, a FRET efficiency of 22% can be obtained for a single donor–acceptor pair [96]. Increasing the number of acceptors to five or more can increase the FRET efficiency to 58% [48, 96].

Although FRET measurements using QDs can convey qualitative molecular association information and appear to have great potential as nanoscale biosensors, there are also a number of limitations with QDs for FRET which should be kept in mind. One major problem is the heterogeneity in QD size which can affect the precision of single-molecule FRET measurements unless the actual spectrum of each individual QD can be measured. QD blinking, which is strongly correlated with spectral jumping (changes in emission peak position), can also significantly affect FRET efficiency and accuracy [103]. Although QDs are superior FRET donors compared with organic dyes, they are not ideal FRET acceptors [104]. Red and NIR QDs are also not optimal for FRET applications due to the long distance between the donor and the acceptor, as well as the limited choice of organic dyes that absorb in this region.

Additional applications of QDs

In addition to the abovementioned studies, QDs have also been used for a variety of other purposes. Herein we highlight some recent literature on novel uses of QDs. A QD ''peptide toolkit'' has been constructed for the creation of small, buffer soluble, mono-disperse peptide-coated QDs with high colloidal stability [47]. QD-based probes have been used for co-immunoprecipitation and Western blot analysis, allowing for simpler and faster image acquisition and quantification than traditional methods (Fig. 4) [105–108]. Since QDs are both fluorescent and electron dense, studies have investigated double- and triple-immunolabeling using light, electron, and correlated microscopy in cells and rodent tissues [109, 110]. Cell-penetrating QDs based on the use of multivalent and endosome-disrupting surface coatings has been reported [111, 112]. Using live HeLa cells, the motion of individual kinesin motors tagged with QDs has been successfully demonstrated [113]. This study demonstrated the importance of single molecule experiments in the investigation of intracellular transport. QD-based optical barcodes can detect single nucleotide polymorpisms where the DNA sequences differ only at a single nucleotide [114, 115]. In comparison with planar chips, bead-based multiplexing has many distinct advantages such as greater statistical analysis, faster assay time, and the flexibility to add additional probes at lower costs [116]. DNA-driven QD arrays have been investigated to utilize photogenerated currents for optoelectronic photoelectrochemistry [117]. QDs have also been used to track RNA interference [118], target surface proteins in living cells [119], detect bacteria [41], and couple with other nanoparticles such as carbon nanotubes [120].

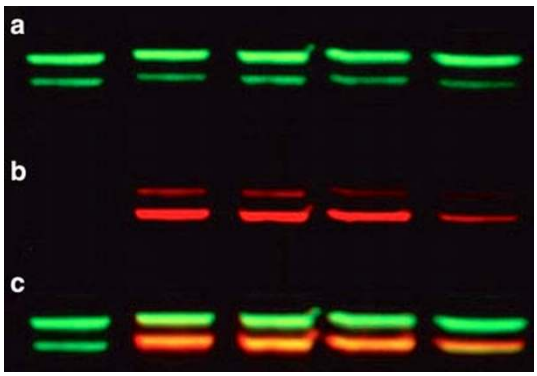

Fig. 4 Western blot of two proteins (**a** & **b**) using two QD-antibody conjugates. Overlay of the two images is shown in **c**. From [107]

Over the last decade, QD-based probes have found numerous applications where fluorescent dyes and proteins were previously the only tools available. QDs have allowed for complicated and difficult multiplexed cellular imaging which was previously impossible given the limitations of fluorescent dyes and proteins. Overall, QD-based probes have almost completely outperformed traditional organic dyes in in vitro and cell-based applications.

QDs for non-targeted imaging in living subjects

One of the primary goals of QD-based research is to eventually translate QDs for use in clinical applications such as in vivo imaging in human subjects. Modeling studies have revealed that two spectral windows exist for QD imaging in living subjects, one at 700–900 nm and another at 1,200–1,600 nm [121]. QDs that emit in the NIR region are suitable for biomedical applications because of low tissue absorption, scattering, and autofluorescence in this region which leads to high photon penetration in tissues [122, 123]. Optically quenched NIR probes based on fluorescent dyes have been employed to detect tumors and have been shown to generate strong signals after enzyme activation by tumor-associated proteases in vivo [124, 125]. NIR QDs provide a superior means to image disease states due to their brightness and photostability in

comparison with commonly used fluorophores. For diagnostic purposes, the wavelength choice of NIR QDs can be matched to the scatter of living tissue for optimal biocompatibility [121, 126]. Significant improvements in QD synthesis, coating, and conjugation techniques combined with their photostability and brightness have made QDs invaluable tools for in vivo imaging. QDs have a large two-photon cross-sectional efficiency 2–3 orders of magnitude greater than that of organic dyes, thus making them well suited for deep-tissue imaging in living subjects using two-photon or time-gated low intensity excitation [73, 127].

Cell trafficking

Individual QDs have been encapsulated in phospholipid block-copolymer micelles for embryo imaging [36]. Micelle encapsulation resulted in great reductions in photobleaching and low non-specific adsorption. After conjugation with DNA, QDs were directly injected into Xenopus embryos and QDs were found to be diffusely distributed throughout the cell during early stages of development while at later stages they mainly resided in cell nuclei. The fluorescence signal of QDs could be followed to the tadpole stage with little or no indication of cytotoxicity. QDs were also reported to have high fluorescent yield and robust photostability for successful imaging of zebrafish embryos [128]. In both studies, QDs were used as contrast agents in living organisms to demonstrate the efficacy of QDs for long-term studies. These findings have provided useful techniques in the fields of embryology, cell biology, as well as disease phenotyping and diagnosis.

QDs have been used as cell markers to study extravasation in small animal models. QD-labeled tumor cells were intravenously injected into live mice and there were no distinguishable differences in behavior between the QD-labeled tumor cells and unlabeled cells [127]. This report successfully showed that QD-labeled tumor cells can permit in vivo imaging despite tissue autofluorescence. These QD-labeled cells could also be used to analyze the distribution of tumor cells in organs and tissues and to track different populations of cells. By using multiphoton laser excitation, five different populations of cells have been simultaneously identified.

Vasculature imaging

Two-photon imaging of vasculature through the skin of living mice has been reported with water-soluble CdSe/ZnS QDs [73]. QDs were dynamically observed in capillaries as deep as several hundred micrometers, and no blinking in solution was observed on the nanosecond to millisecond time scale. Compared to conventional methods using 70-kD FITC-dextran, QDs provided significantly more information at the same depth. In another report, coronary vasculature was imaged in vivo and the effects of tissue absorbance, scatter, and thickness on the performance of QDs were analyzed when embedded in biological tissue [121]. Theoretical modeling suggested that optimal spectral windows for in vivo imaging exist at 700–900 nm and 1200–1600 nm. Using multiphoton microscopy, QDs can differentiate tumor vessels from perivascular cells and matrix better than traditional fluorescently-labeled dextran vessel markers (Fig. 5) [129]. Multiphoton microscopy through gradient index lenses has also been used for minimally invasive, subcellular resolution imaging of cortical layer V and hippocampus several millimeters deep in anesthetized live animals [130].

NIR CdMnTe/Hg QDs have been used for deep-tissue in vivo optical imaging [131]. QDs were grown in aqueous solution and coated with bovine serum albumin. After either subcutaneous or intravenous injection, these QDs were used as angiographic contrast agents for vessels sur-

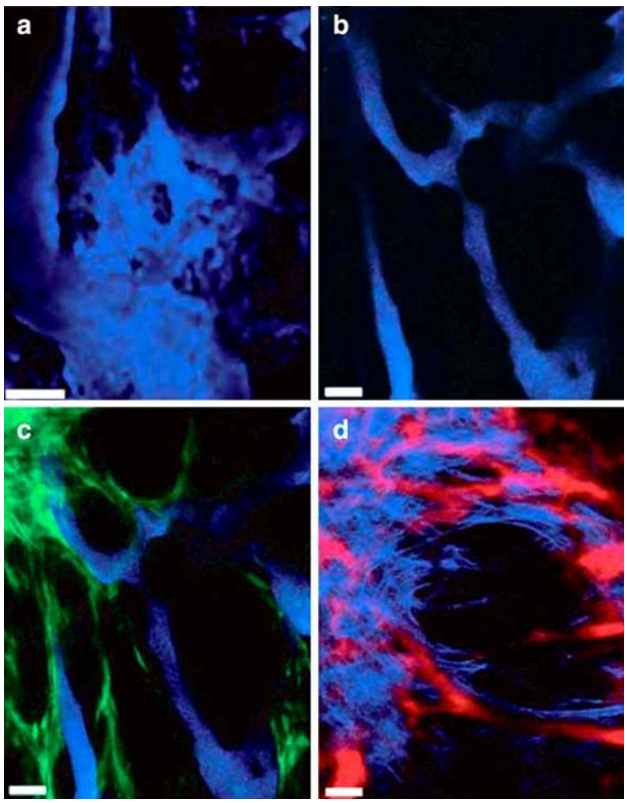

Fig. 5 Vasculature imaging with QDs. (**a**) Fluorescently labeled dextran gave blurred images of tumor vessels. (**b**) QD imaging yielded a sharp boundary between the vessel and interstitium. (**c**) Concurrent imaging of both QD and GFP (green) provides clear separation of the vessel from GFP-expressing perivascular cells. (**d**) Vessels highlighted with QD (red) were imaged simultaneously with the second harmonic generation signal from collagen (blue). Scale bar = 50 μm. From [129]

rounding and penetrating murine squamous cell carcinoma in mice. No significant photobleaching or degradation of QDs was observed even after an hour of continuous excitation. The stability of QDs combined with their time resolution of optical detection makes them attractive candidates for pharmacokinetic imaging studies.

Visualization of blood vessels in the chick chorioallantoic membrane, a popular model for studying various aspects of blood vessel development such as angiogenesis, was recently achieved with QDs [132]. Intravitally injected QDs were biocompatible and stayed in circulation for over four days without any observed deleterious effects. The vascular residence time was adjustable through different QD surface modifications. QDs with longer emission wavelengths (>655 nm) virtually eliminated all chick-derived autofluorescence. In comparison with FITC-dextran, QDs were able to image vessels as well as or better than FITC-dextran at 2–3 orders of magnitude lower concentration. QDs were also fixable with low fluorescence loss, allowing for further sample analysis when used in conjunction with histological processing.

Lymph node mapping

Lymph node imaging with QDs has been reported in living subjects. Type-II QDs, in which both the valence and conduction bands in the core are lower (or higher) than those in the shell, have tunable fluorescence emission while preserving the absorption cross-section [133]. NIR type-II CdTe/CdSe QDs (850 nm emission) were injected intradermally into live mice and pigs [24]. These QDs rapidly migrated to local sentinel lymph nodes (SLNs) and were imaged virtually background-free, allowing image-guided resection of a one centimeter deep lymph node in a pig (Fig. 6). Imaging the lymph nodes one centimeter deep in tissue required only 5 mW/cm^2 of excitation. This study is the first demonstration of NIR QD-guided surgery, which takes advantage of both the spectroscopic properties and the relatively large size (>10 nm) of QDs. SLN mapping is clinically important since these are the sites where metastatic cancer cells are often found. Intraoperative SLN mapping in various locations of the body has also been reported in adult pigs [134–136], where only 200 pmol of QDs was needed and these QDs quickly and accurately mapped lymphatic drainage and SLNs. Many other SLN mapping experiments have also been reported in mice [137, 138] and rats [139–141]. SLN mapping using QDs overcomes the limitations of currently available methods and provides highly sensitive, real-time image-guided dissection, which may permit potential mapping of SLNs and lymphatic flow in patients.

Simultaneous two-color in vivo wavelength-resolved spectral fluorescence lymphangiography using two NIR QDs with different emission spectra has been reported [142]. This study may provide insight into the mechanisms of drainage from different lymphatic basins that may lead to SLN detection of breast cancer as well as prevention of complications such as lymphedema of the extremities. Recently, it was demonstrated that QDs injected into model tumors rapidly migrated to SLNs [143]. PEG-coated QDs with terminal carboxyl, amino, or methoxyl groups all similarly migrated from the tumor to surrounding lymph nodes. Passage from the tumor through lymphatics to adjacent nodes could be dynamically visualized through the skin and at least two nodes could be typically defined. Imaging during necropsy confirmed QD confinement to the lymphatic system and demonstrated tagging of SLNs for pathology. Examination of the SLNs identified by QD localization showed that several of them contained metastatic tumor foci.

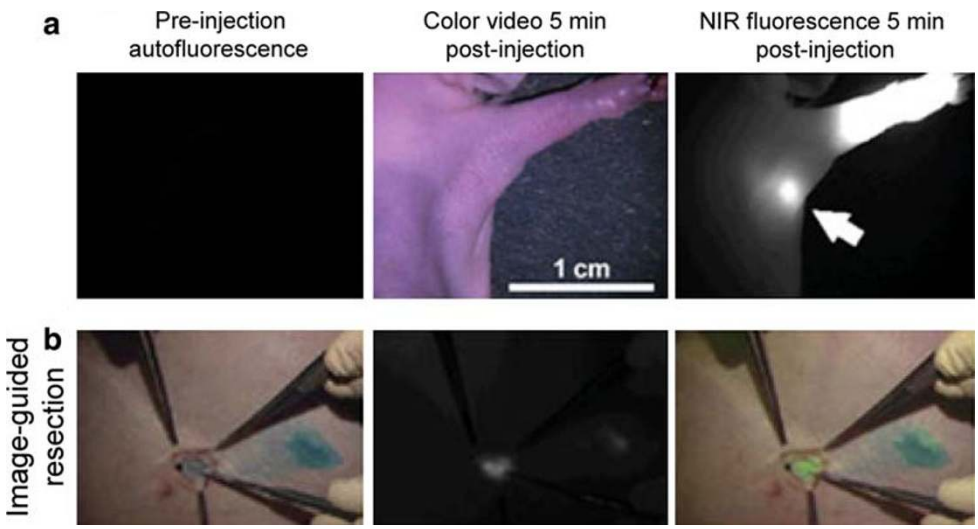

Fig. 6 Sentinel lymph node mapping using QDs. (**a**) Images of a mouse injected intradermally with type II NIR QDs in the left paw. (**b**) Image guided resection of a lymph node in a pig. From [24]

Neural imaging

Diffusion within the extracellular space (ECS) of the brain is necessary for chemical signaling and for neurons and glia to access nutrients and therapeutic agents [144, 145]. Integrative optical imaging was employed to show that water-soluble QDs diffuse within the ECS of adult rat neocortex in vivo [146]. This report could improve the modeling of neurotransmitter spread after spillover and ectopic release while establishing size limits for diffusion of drug delivery vectors such as viruses, liposomes, and nanoparticles in brain ECS.

Intravenously injected QDs were shown to be taken up by macrophages and localize to experimental glioma in a rat model using optical detection [147]. Initial QD injections were performed at a concentration of 6.8 μM in a volume of 500 μL, which is more than 15 times the dose injected for SLN mapping in a 35 kg adult pig (2,100 times based on the animal body weight) [134–136]. It was determined that an increase in concentration and volume may help QDs avoid early sequestration by the reticuloendothelial system (RES; e.g. lymph nodes, liver, spleen, and bone marrow [148]) and provide a better chance for glioma uptake of QDs. Further increases in the injected QD dose by three fold resulted in detectable fluorescence signals in the rat brain [149, 150]. Although it is suggested that these techniques have the potential to be translated into clinical use in humans allowing QDs to optically guide brain tumor biopsies and resections, the enormous amount of QDs needed to generate detectable signal in the tumor is a major concern in terms of both toxicity and cost.

Surface coating and the in vivo behavior of QDs

Coating QDs with high molecular weight poly(ethylene glycol) (PEG) molecules can reduce QD accumulation in the liver and bone marrow [151]. QDs with different length PEG coatings were tested using light and electron microscopy on tissue sections and noninvasive whole-body fluorescence imaging. QDs were found to remain stable in the bone marrow and lymph nodes of animals after several months, demonstrating their high stability without interfering with normal cell physiology and cell differentiation.

Extensive study of different QD surface coatings revealed important insights for future design of QD-based probes and experimental setups [151, 152]. First, QDs are easily visible through the skin of nude mice using NIR QDs. The excitation wavelength is also important in determining how deep QDs may be observed. Second, carboxyl-coated QDs are rapidly taken up by the RES while amino-terminal PEG-coated QDs have varying half-lives in circulation depending on the molecular weight of PEG. Third, when using neutral methoxy-terminated PEG

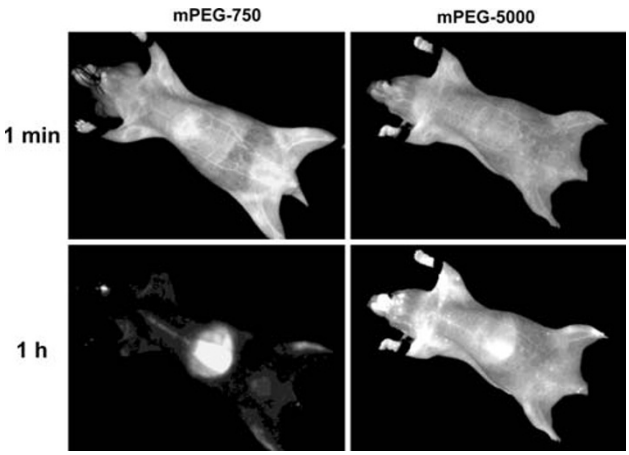

Fig. 7 Different surface coating of QDs results in different in vivo kinetics. mPEG-750 coated QDs circulates much shorter than mPEG-5000 coated QDs. Even at 1 min, significant liver uptake of mPEG-750 QDs is visible. At 1 h, mPEG-750 QDs completely cleared from the circulation while mPEG-5000 QDs persisted. From [151]

(mPEG) coating, results vary depending on the length of the PEG and the degree of substitution. Highly substituted QDs yielded half-lives in the 3- to 8-h range for mPEG-5000 coated QDs (Fig. 7). Increasing the PEG size to 10 kD or 20 kD produced no further improvement in the circulation half-life. Fourth, sites of deposition vary with the QD surface coating. Amino-PEG, carboxy-PEG, and mPEG-700 coated QDs are all deposited in the RES with sites slightly varying. Deposition of uncharged PEG coated QDs depended on the molecular size of the PEG and on the density of substitution. Most importantly, the injected dose of all types of QDs tested in these studies was excreted in the feces within 1–2 days.

In vivo targeted imaging using QDs

In order to make QDs more useful for in vivo imaging and other biomedical applications, QDs need to be effectively, specifically, and reliably directed to a specific organ or disease site without alteration. Specific targeting can be obtained by attaching targeting molecules to the QD surface. However, in vivo targeting and imaging is very challenging due to the relatively large overall size (typically about 20 nm in diameter) and short circulation time of QD conjugates. To date, there have been only a handful of successful reports in the literature.

Peptide-conjugated QDs

The first report to demonstrate in vivo targeting of QD conjugates employed peptides as the targeting ligands [46]. Peptide-conjugated QDs were injected intravenously into

MDA-MB-435 breast carcinoma xenograft-bearing nude mice. Three peptides were tested: CGFECVRQCPERC (denoted as GFE) which binds to membrane dipeptidase on the endothelial cells [153, 154], KDEPQRRSARLSAK-PAPPKPEPKPKKAPAKK (denoted as F3) which preferentially binds to blood vessels and tumor cells in various tumors [155], and CGNKRTRGC (denoted as LyP-1) which recognizes lymphatic vessels and tumor cells in certain tumors [156]. Since the QD used in this study emits in the visible range which is not optimal for in vivo imaging, ex vivo histological analysis were carried out to show that QDs were specifically directed to the tumor vasculature and organ targets by the surface peptide molecules. A high level of PEG substitution on the QDs was found to be important to reduce non-selective accumulation in the RES, thereby increasing the circulation half-life and targeting efficiency. QD-F3 colocalizes with blood vessels in tumor tissue and QD-LyP-1 also accumulated in tumor tissue but did not colocalize with the blood vessel marker. QD-F3 and QD-LyP-1 (of different emission wavelength) injected into the same tumor mouse targeted different structures in the tumor tissue, showing that QDs can be targeted in vivo with a high level of specificity. This pioneering report first demonstrated the feasibility of specific targeting of QD in vivo and opened up a new field of QD-based research.

We reported the first in vivo targeted imaging of tumor vasculature using peptide-conjugated QDs [45]. Cell adhesion molecule integrin $\alpha_v\beta_3$ is highly expressed on activated endothelial cells and tumor cells but is not readily detectable in resting endothelial cells and most normal organ systems [157, 158]. Previous reports have demonstrated that integrin $\alpha_v\beta_3$ is an excellent tumor-related target [157–165]. The fact that integrin $\alpha_v\beta_3$ is over-expressed on both tumor vasculature and tumor cells makes it a prime target for in vivo targeted imaging using QDs, as extravasation is not required to observe tumor signal. Arginine–glycine–aspartic acid (RGD; potent integrin $\alpha_v\beta_3$ antagonist) containing peptides were conjugated to QD705 (emission maximum at 705 nm) and QD705-RGD exhibited high affinity integrin $\alpha_v\beta_3$ specific binding in cell culture and ex vivo. In vivo NIR fluorescence (NIRF) imaging was carried out on athymic nude mice bearing subcutaneous integrin $\alpha_v\beta_3$-positive U87MG human glioblastoma tumors (Fig. 8) [45]. Tumor fluorescence intensity reached a maximum at 6 h post-injection with good contrast. The size of QD705-RGD (~20 nm) prevented efficient extravasation, thus QD705-RGD mainly targeted tumor vasculature instead of tumor cells. Immunofluorescence staining of the tumor vessels confirmed that the majority of the QD fluorescence signal in the tumor colocalizes with the tumor vessels. Successful in vivo tumor imaging using QD conjugates has introduced new perspectives for targeted NIRF imaging and may aid in cancer detection and management including image-guided surgery. This probe may also have great potential as a universal NIRF probe for detecting tumor vasculature in living subjects.

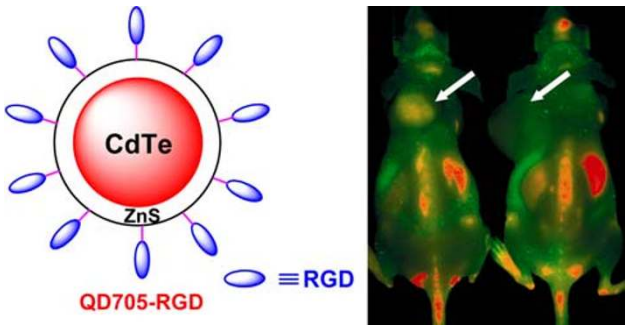

Fig. 8 RGD Peptide-conjugated QD705 successfully targets the tumor vasculature in vivo. Mouse on the left was injected with QD705-RGD and the mouse on the right was injected with QD705. Arrows indicate tumors. From [45]

Antibody-conjugated QDs

QD-based probes can be delivered to tumors through either passive or active targeting mechanisms in living subjects. In passive targeting, macromolecules and nanometer-sized particles can accumulate in the tumor through enhanced permeability and retention (EPR) effects [166, 167]. Angiogenic tumors produce vascular endothelial growth factor [168–170], which hyperpermeabilizes tumor neovasculature and causes leakage of circulating macromolecules and nanoparticles. Subsequent macromolecule or nanoparticle accumulation occurs since tumors lack an effective lymphatic drainage system.

ABC triblock copolymer-coated QDs for prostate cancer targeting and imaging in live animals has been reported [37]. Research has identified prostate-specific membrane antigen (PSMA) as a cell-surface marker for both prostate epithelial cells and neovascular endothelial cells [171]. Polymer-coated QDs were conjugated to PSMA-specific monoclonal antibodies and it was estimated that there were 5–6 antibody molecules per QD. Using spectral imaging techniques where fluorescence signals from QDs and mouse autofluorescence can be separated based on the emission spectra [172, 173], intravenously injected probe were found to accumulate in the tumor site (Fig. 9) [37]. Multiplexed imaging was also demonstrated in live animals using QD-labeled cancer cells. Since no histological analysis was carried out to investigate the expression level of PSMA on the tumor cells and tumor vasculature, it was unclear whether these QD conjugates targeted tumor vasculature or tumor cells. In addition, the QDs used in this

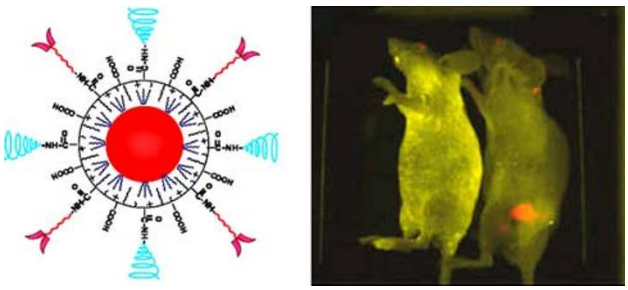

Fig. 9 Antibody-conjugated QDs for in vivo cancer targeting and imaging. Mouse on the left was a control. From [37]

study were not optimized for tissue penetration or imaging sensitivity because the emission wavelength was in the visible region instead of the NIR region.

In a recent study, QDs were linked to anti-AFP (alpha-fetoprotein, a marker for hepatocellular carcinoma cell lines) antibody for in vivo tumor targeting and imaging [174]. No in vitro validation of the QD probe was carried out before the in vivo experiments. It was reported that active tumor targeting and spectroscopic hepatoma imaging was achieved using an integrated fluorescence imaging system. The heterogeneous distribution of the QD-based probe in the tumor was also evaluated by a site-by-site measurement method. A major flaw of this study is that it was not shown whether or not the anti-AFP antibody was actually attached to the QD. Therefore, there is not enough experimental evidence to support the conclusion that the tumor contrast observed was from active rather than passive targeting.

Tracking a single QD conjugated with tumor-targeting antibody in tumors of living mice was achieved using a dorsal skinfold chamber and a high-speed confocal microscope with a high-sensitivity camera [175]. QDs labeled with anti-HER2 monoclonal antibody were injected into mice bearing HER2-overexpressing breast cancer to analyze the molecular processes of its tumor delivery. Movement of a single QD-antibody conjugate (total number of QD particles injected was ~1.2×10^{14}) was observed at 30 frames per second inside the tumor through the dorsal skinfold chamber. QDs were observed during six processes of delivery: in a blood vessel, during extravasation, in the extracellular region, binding to HER2 on the cell membrane, moving from the cell membrane to the perinuclear region, and in the perinuclear region. The movement of the QD-antibody conjugate at each stage followed a ''stop and go'' pattern. Despite the technical difficulty of this experiement, no information was obtained regarding the percentage of intravenously injected QDs that extravasated. Therefore, little can be concluded about the overall behavior of such QD-antibody conjugates in vivo. It was unclear whether the ''stop and go'' pattern is typical for the majority of injected QD conjugates or if it is only limited to a small subset of QDs. It is likely that the majority of the QD conjugates were taken up by the RES shortly after injection and that only certain QD conjugates such as the smallest particles actually extravasated.

Recent advances in QD technology

Bioluminescence resonance energy transfer (BRET)

QDs have shown great potential for molecular imaging and cellular investigations of biological processes. However, the requirement for external light excitation can partially offset the favorable tissue penetration properties of NIR QDs. This type of excitation also results in significantly increased background autofluorescence. The use of direct bioluminescence light to excite QDs has partially overcome this problem [176]. Luciferases have been widely used as reporter genes in biological research [177, 178]. However, the bioluminescence activity of commonly used luciferases is too labile in serum. Specific mutations of Renilla luciferase, selected using a consensus sequence driven strategy, were screened for their ability to confer stability of activity in serum as well as their light output [179]. A mutant Renilla luciferase with eight mutations (RLuc8) was selected with a 200-fold increase in resistance to inactivation in murine serum and a 4-fold increase in light output. Multiple molecules of RLuc8 were covalently conjugated to a single fluorescent QD, forming a conjugate about 22 nm in hydrodynamic diameter (Fig. 10) [176]. When RLuc8 bound its substrate coelenterazine, it converted chemical energy into photon energy and emitted broad spectrum blue light peaking at 480 nm. Due to the complete overlap of the RLuc8 emission and QD absorption spectra, QDs were efficiently excited in the absence of external light. In vivo imaging showed greatly enhanced signal-to-background ratio after injection of the QD-RLuc8 conjugate into the blood stream. RLuc8 can serve as a

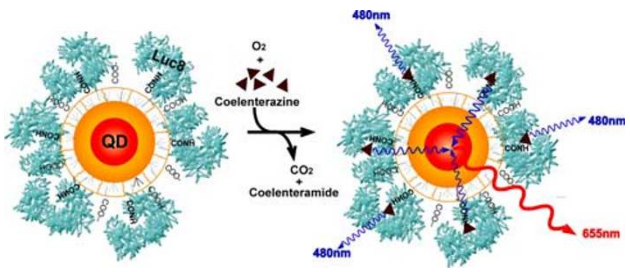

Fig. 10 Self-illuminating QDs based on bioluminescence resonance energy transfer. From [176]

BRET donor for virtually any QDs and these probes can be used for multiplexed imaging. BRET has the potential to greatly improve NIRF detection in living tissue and similar QD conjugates can be obtained when RLuc8 is fused to other proteins, thus enabling new possibilities for imaging biological events [180]. One of the major goals BRET will have to achieve before it can be widely used for in vivo imaging is targeting specificity. Since there are many RLuc8 molecules on the QD surface which cover the majority of the QD surface area, it remains to be tested whether there will be enough space left to attach enough ligands for desirable targeting efficacy.

Non-Cd based QDs

There have been many serious questions and concerns raised regarding the cytotoxicity of inorganic QDs containing Cd, Se, Zn, Te, Hg, and Pb [181–184]. These chemicals can be potent toxins, neurotoxins, and/or teratogens depending on the dosage, complexation, and accumulation in the liver and the nervous system. At very low doses, these metals are bound by metallothionein proteins and may be excreted slowly or sequestered in vivo in adipose and other tissues [181, 185]. Cadmium has a half-life of about 20 years in humans and it is a suspected carcinogen that can accumulate in the liver, kidney, and many other tissues since there is no known active mechanism to excrete cadmium from the human body [186]. Although many studies have found no adverse effects of QDs on cell viability, morphology, function, or development over the duration of experiments (hours to days) at concentrations optimized for labeling efficiency [36, 38, 63, 127], the cellular toxicity of QDs under extreme conditions such as photo-oxidation and strong UV excitation has been clearly demonstrated [185, 187]. In general, the less protected the QD core or core/shell is, the sooner the appearance of signs of interference with cell viability or function as a result of Cd^{2+} and/or Se^{2-} release. Thick ZnS overcoating (4–6 monolayers) in combination with efficient surface capping has been shown to substantially reduce desorption of core ions and make QDs more biologically inert [185]. Interestingly, the toxicity of QDs has been utilized for photodynamic therapy applications such as tumor ablation [188, 189]. As QD technology evolves and brighter probes are created with improved detection efficiency, the easiest way to decrease cytotoxic effects would be to use lower quantities of QDs. In many cases, the amount of free Cd^{2+} ions released by QDs is far below the dose needed to cause cadmium poisoning in animal models.

InAs-based QDs can be a substitute for Cd-based QDs with lower cytotoxicity [138, 190, 191]. The amount of As used is estimated to be hundreds of times lower than the dose of As_2O_3 used to treat human leukemia. Mn- or Cu-doped zinc chalcogenide QDs have been reported and can cover a similar emission window as that of CdSe QDs [192, 193]. Besides the low toxicity by replacing Cd with Zn, such QDs are also less sensitive to environmental changes such as thermal, chemical, and photochemical disturbances. These doped QDs have color-tunability with good quantum efficiency and are promising candidates for future efforts to lower QD-based cytotoxicity. They also have narrow emission spectra (45–65 nm full width at half maximum) and can cover most of the visible spectral window. In the near future, it is expected that doped QDs that emit in the NIR region will be developed. Extensive scrutiny and research into the toxicity profiles will be needed before QDs can be employed in any medical procedures. In addition, further studies are also needed to investigate the clearance mechanism of QDs from living systems.

Moving towards smaller QDs

For inorganic nanoparticles such as QDs, the particle size and shape is relatively rigid compared to other organic nanoparticles such as dendrimers. To date, most of the QDs evaluated in vivo are 15 nm or more in hydrodynamic diameter. Although tumor vasculature is typically quite leaky, such size does not permit efficient extravasation. It is expected that with smaller sizes, QDs will extravasate more efficiently and give more efficient in vivo targeting of both tumor vasculature and tumor cells. Smaller sized QDs are also expected to have lower RES uptake which will translate into better image quality. Different core/shell structures and thinner polymer coating has been reported to reduce the overall size of QDs [137, 193], and unusually small, water soluble QDs composed of InAs/ZnSe (core diameter < 2 nm) have been developed [137]. Although these QDs have lower quantum yield (<10%), the smaller size is attractive for imaging applications. These unusually small QDs were not trapped in SLNs, bur rather they migrated into the lymphatic system and the channels between the nodes. In addition, these small QDs could also migrate out of the blood vessels and into the interstitial fluid.

Dendron-coated QDs have high stability, versatility, and chemical/biochemical proccessibility [194, 195]. Unlike the typical polymer coating, dendron-ligands are tight and small in radial dimension, resulting in an overall smaller size of QDs (Fig. 11). The surface density and length of the PEG units on the outer surface of the resulting dendron-coated QDs can be varied by synthesizing dendron ligands with different terminal structures. A ‘‘peptide toolkit’’ has been reported which can provide a straightforward means for improving biocompatibility for cell biology and in vivo applications [47]. In the future, it is likely that small

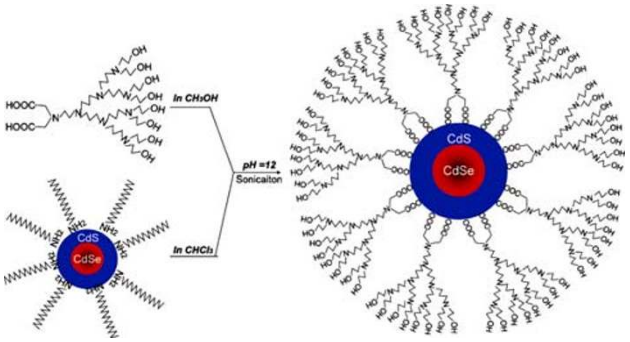

Fig. 11 Schematic illustration of the formation of dendron-coated QDs. From [195]

molecule or peptide-coated QDs will have better opportunities for development and expansion in in vivo applications than protein or antibody-conjugated QDs.

Multifunctional probes

Among all of the molecular imaging modalities currently available, no single modality is perfect and sufficient to obtain all the necessary information [196]. Due to the current obstacles in fluorescence tomography [197–199], it is difficult to adequately quantify QD signal in living subjects based on fluorescence intensity alone, particularly in deep tissues. Combining QD-based imaging with 3D tomography techniques such as positron emission tomography (PET), single photon emission computed tomography (SPECT), and magnetic resonance imaging (MRI) can permit the elucidation of targeting mechanisms, biodistribution, and dynamics in living animals with higher sensitivity and/or accuracy. One of the most promising applications for QDs is the development of multifunctional QD-based probes for multimodality molecular imaging in vitro and in vivo. A multimodality approach would make it possible to image targeted QDs at all scales, from whole-body down to nanometer resolution, using a single probe.

A series of core/shell CdSe/$Zn_{1-x}Mn_xS$ nanoparticles have been synthesized for use in both optical imaging and MRI [200]. Mn^{2+} content was in the range of 0.6–6.2% and varies with the thickness of the shell or amount of Mn^{2+} introduced to the reaction. The quantum yield and Mn^{2+} concentration in the nanoparticles were sufficient to produce contrast for both modalities at a relatively low concentration. Bifunctional nanocomposite systems consisting of Fe_2O_3 magnetic nanoparticles and CdSe QDs have been synthesized [201]. QDs can be coated with paramagnetic and pegylated lipids for use as detectable and targeted probes with MRI [202]. These QDs are useful as dualmodality contrast agents due to their high relaxivity and

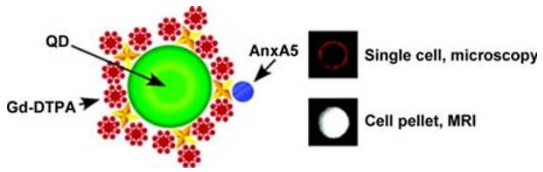

Fig. 12 A QD-based probe for both fluorescence imaging and MRI. From [204]

ability to retain their optical properties. Several other QD-based probes for both fluorescence imaging and MRI have also been reported (Fig. 12) [202–204]. Polymer-coated Fe_2O_3 cores overcoated with a CdSe-ZnS QD shell and functionalized with antibodies have been used to magnetically capture breast cancer cells and view them with fluorescence imaging [205]. Magnetic QDs composed of CdS-FePt have also been synthesized [206].

QDs have relatively large surface areas which can be conjugated with more than one targeting ligand. Novel tumor-specific antibody fragments, growth factors, peptides, and small molecules can be attached to QDs for the delivery of QDs to tumors in vivo for multi-parameter imaging of biomarkers, with the ultimate goal of guiding therapy selection and predicting response to therapy. This nano-platform approach will enable detection and measurement of many biomarkers simultaneously which may lead to better signal/contrast than QDs modified with only one type of targeting ligand. The ability to accurately assess the pharmacokinetics and tumor targeting efficacy of the biologically modified QDs is of crucial importance to assess future multitargeting (to target multiple targets with the same QD) and eventually multiplexing (to target multiple targets simultaneously using QDs of different emission wavelengths) studies. Dualmodality PET/NIRF imaging probe offers synergistic advantages over the single modality imaging probe by overcoming the difficulty of quantifying fluorescence intensity in vivo and ex vivo. For the first time, we quantitatively evaluated the tumor targeting efficacy of dualfunctional QD-based probes using both NIRF and PET imaging (Fig. 13) [207]. Both RGD peptides and macrocyclic chelator DOTA were conjugated to QD705. RGD peptides can allow for integrin $\alpha_v\beta_3$ targeting and DOTA can complex ^{64}Cu (a positron emitter with 12.7 h half-life) to enable PET imaging [160, 208, 209]. Non-invasive PET imaging using radiolabeled QD conjugates can provide a robust and reliable measure of the in vivo biodistribution of QDs. With further improvement in QD technology, it is expected that accurate evaluation of the in vivo tumor targeting efficacy using quantitative imaging modalities (e.g. PET) will greatly facilitate future biomedical applications of QDs. Such information will also be critical for fluorescence-guided surgery by sensitive,

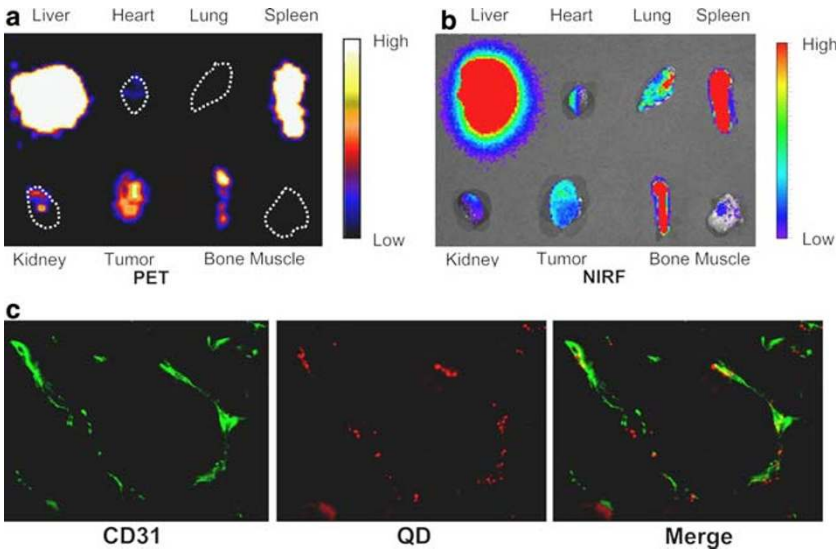

Fig. 13 Dualfunctional QD-based probe for both PET and NIRF imaging. (**a**) PET image of harvested major organs/tissues at 5 h post-injection of the dualfunctional probe. (**b**) NIRF image of harvested major organs/tissues at 5 h post-injection of the probe. (**c**) Immunofluorescence staining of the tumor tissue revealed that QDs are targeting the tumor vasculature. From [207]

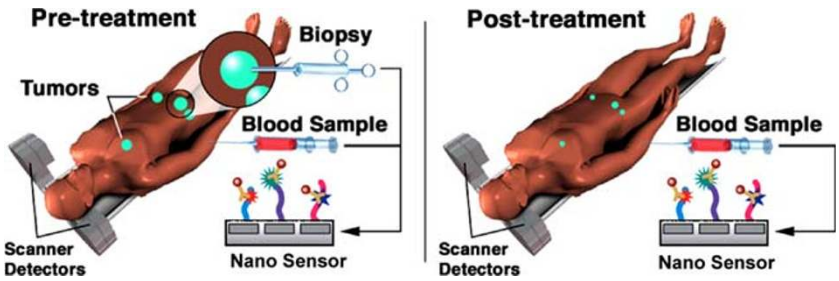

Fig. 14 Patients can have their tumors biopsied and blood samples drawn for protein profiling by ex vivo nanosensors to predict their response to a given therapy. In addition, they will also be imaged with molecular imaging probes of different types to predict their response. Post-treatment and potentially during treatment, patient response will be evaluated by blood analysis and molecular imaging to ensure the accurate differentiation of responders from non-responders.

specific, and real-time intraoperative visualization of molecular features of normal and disease processes.

Conclusion and perspectives

QDs as biological probes have lived up to much of their initially promoted potential for in vitro and in vivo imaging. Since the first demonstration of QDs for biological applications [1, 2], numerous breakthroughs in QD technology have led to the recent success of in vivo targeted imaging of QDs in live animals [37, 45]. Future development of improved QD-based biological probes for in vivo optical imaging is promising for both basic science and clinical applications.

Nanotechnology has the potential to significantly impact cancer diagnosis and cancer patient management. QD-based ex vivo protein nanosensors (e.g. FISH, FRET) and in vivo imaging are both critical for future optimization in cancer management. Ex vivo diagnostics in combination with in vivo diagnostics can markedly impact future cancer patient management by providing a synergistic approach that neither strategy can provide alone. After further development and validation, QD-based approaches (both ex vivo nanosensor and in vivo imaging) will eventually be able to predict which patients will likely respond to a specific anticancer therapy and monitor their response to personalized therapy (Fig. 14). With their capacity to provide enormous sensitivity, throughput, and flexibility, QDs have the potential to profoundly impact cancer patient management in the future.

QD-based tumor imaging in mice can not be directly scaled up to in vivo imaging in human applications due to limited optical signal penetration depth. In clinical settings, optical imaging is relevant for tissues close to the surface of the skin, tissues accessible by endoscopy, and intraoperative visualization. NIR optical imaging devices for detecting and diagnosing breast cancer have been tested in patients and the initial results are encouraging [210, 211]. Multiple wavelength QDs emitting in the NIR region can

allow for multiplexed imaging of deeper tissues, thus significantly extending potential human applications. QD-based multitarget imaging can also play an important role in optically guided surgery in the future. Overall, the major roadblocks for clinical translation of QDs are inefficient delivery, toxicity, and lack of quantification. However, with the development of smaller non-Cd based multifunctional QDs and further improvement on conjugation strategy, it is expected that QDs will achieve optimal tumor targeting efficacy with acceptable toxicity profile for clinical translation in the near future using either NIRF imaging alone or multimodality imaging.

Acknowledgements The authors would like to thank the National Institute of Biomedical Imaging and Bioengineering (NIBIB) (R21 EB001785), NCI (R21 CA102123, P50 CA114747, U54 CA119367, R24 CA93862), Department of Defense (DOD) (W81XWH-04–1-0697, W81XWH-06-1-0665, W81XWH-06-1-0042, W81XWH-07-1-0374, DAMD17-03-1-0143), Benedict Cassen Postdoctoral Fellowship from the Education and Research Foundation of the Society of Nuclear Medicine (to W.C.), and Stanford University School of Medicine Medical Scholars Program (to A.R.H.).

References

1. M. Bruchez Jr., M. Moronne, P. Gin, S. Weiss, A.P. Alivisatos, Science **281**, 2013 (1998)
2. W.C. Chan, S. Nie, Science **281**, 2016 (1998)
3. Z. Liu, W. Cai, L. He, N. Nakayama, K. Chen, X. Sun, X. Chen, H. Dai, Nat. Nanotechnol. **2**, 47 (2007)
4. Y. Cui, C.M. Lieber, Science **291**, 851 (2001)
5. L.R. Hirsch, R.J. Stafford, J.A. Bankson, S.R. Sershen, B. Rivera, R.E. Price, J.D. Hazle, N.J. Halas, J.L. West, Proc. Natl. Acad. Sci. USA **100**, 13549 (2003)
6. P. Grodzinski, M. Silver, L.K. Molnar, Expert Rev. Mol. Diagn. **6**, 307 (2006)
7. A.G. Cuenca, H. Jiang, S.N. Hochwald, M. Delano, W.G. Cance, S.R. Grobmyer, Cancer **107**, 459 (2006)
8. M. Ferrari, Nat. Rev. Cancer **5**, 161 (2005)
9. E.S. Kawasaki, A. Player, Nanomedicine **1**, 101 (2005)
10. A. Miyawaki, A. Sawano, T. Kogure, Nat. Cell Biol. Suppl, S1 (2003)
11. Al.L. Efros, A.L. Efros, Sov. Phys. Semicond. **16**, 772 (1982)
12. A.I. Ekimov, A.A. Onushchenko, Sov. Phys. Semicond. **16**, 775 (1982)
13. V.V. Milanovic, Z. Ikonic, Phys. Rev. B **39**, 7982 (1989)
14. W.C. Chan, D.J. Maxwell, X. Gao, R.E. Bailey, M. Han, S. Nie, Curr. Opin. Biotechnol. **13**, 40 (2002)
15. B.O. Dabbousi, J. RodriguezViejo, F.V. Mikulec, J.R. Heine, H. Mattoussi, R. Ober, K.F. Jensen, M.G. Bawendi, J. Phys. Chem. B **101**, 9463 (1997)
16. M. Dahan, T. Laurence, F. Pinaud, D.S. Chemla, A.P. Alivisatos, M. Sauer, S. Weiss, Optics Lett. **26**, 825 (2001)
17. X. Michalet, F. Pinaud, T.D. Lacoste, M. Dahan, M.P. Bruchez, A.P. Alivisatos, S. Weiss, Single Mol. **2**, 261 (2001)
18. P. Alivisatos, Nat. Biotechnol. **22**, 47 (2004)
19. C.J. Murphy, Anal. Chem. **74**, 520A (2002)
20. X. Michalet, F.F. Pinaud, L.A. Bentolila, J.M. Tsay, S. Doose, J.J. Li, G. Sundaresan, A.M. Wu, S.S. Gambhir, S. Weiss, Science **307**, 538 (2005)
21. I.L. Medintz, H.T. Uyeda, E.R. Goldman, H. Mattoussi, Nat. Mater. **4**, 435 (2005)
22. Z.B. Li, W. Cai, X. Chen, J. Nanosci. Nanotechnol. **7**, in press (2007)
23. A.J. Nozik, Annu. Rev. Phys. Chem. **52**, 193 (2001)
24. S. Kim, Y.T. Lim, E.G. Soltesz, A.M. De Grand, J. Lee, A. Nakayama, J.A. Parker, T. Mihaljevic, R.G. Laurence, D.M. Dor, L.H. Cohn, M.G. Bawendi, J.V. Frangioni, Nat. Biotechnol. **22**, 93 (2004)
25. C.B. Murray, D.J. Norris, M.G. Bawendi, J. Am. Chem. Soc. **115**, 8706 (1993)
26. Z.A. Peng, X. Peng, J. Am. Chem. Soc. **123**, 183 (2001)
27. M.A. Hines, P. Guyotsionnest, J. Phys. Chem. **100**, 468 (1996)
28. X.G. Peng, M.C. Schlamp, A.V. Kadavanich, A.P. Alivisatos, J. Am. Chem. Soc. **119**, 7019 (1997)
29. R.E. Bailey, S. Nie, J. Am. Chem. Soc. **125**, 7100 (2003)
30. J.M. Tsay, M. Pflughoefft, L.A. Bentolila, S. Weiss, J. Am. Chem. Soc. **126**, 1926 (2004)
31. X. Peng, L. Manna, W. Yang, J. Wickham, E. Scher, A. Kadavanich, A.P. Alivisatos, Nature **404**, 59 (2000)
32. W.W. Yu, E. Chang, R. Drezek, V.L. Colvin, Biochem. Biophys. Res. Commun. **348**, 781 (2006)
33. H.T. Uyeda, I.L. Medintz, J.K. Jaiswal, S.M. Simon, H. Mattoussi, J. Am. Chem. Soc. **127**, 3870 (2005)
34. W.J. Parak, Nanotechnology **14**, R15 (2003)
35. T. Nann, P. Mulvaney, Angew. Chem. Int. Ed. Engl. **43**, 5393 (2004)
36. B. Dubertret, P. Skourides, D.J. Norris, V. Noireaux, A.H. Brivanlou, A. Libchaber, Science **298**, 1759 (2002)
37. X. Gao, Y. Cui, R.M. Levenson, L.W.K. Chung, S. Nie, Nat. Biotechnol. **22**, 969 (2004)
38. X. Wu, H. Liu, J. Liu, K.N. Haley, J.A. Treadway, J.P. Larson, N. Ge, F. Peale, M.P. Bruchez, Nat. Biotechnol. **21**, 41 (2003)
39. J.C. Sheehan, P.A. Cruickshank, G.L. Boshart, J. Org. Chem. **26**, 2525 (1961)
40. M. Bodanszky, Pept. Res. **5**, 134 (1992)
41. R. Edgar, M. McKinstry, J. Hwang, A.B. Oppenheim, R.A. Fekete, G. Giulian, C. Merril, K. Nagashima, S. Adhya, Proc. Natl. Acad. Sci. USA **103**, 4841 (2006)
42. M. Dahan, S. Levi, C. Luccardini, P. Rostaing, B. Riveau, A. Triller, Science **302**, 442 (2003)
43. D. Marshall, R.B. Pedley, J.A. Boden, R. Boden, R.G. Melton, R.H. Begent, Br. J. Cancer **73**, 565 (1996)
44. S.J. Rosenthal, I. Tomlinson, E.M. Adkins, S. Schroeter, S. Adams, L. Swafford, J. McBride, Y. Wang, L.J. DeFelice, R.D. Blakely, J. Am. Chem. Soc. **124**, 4586 (2002)
45. W. Cai, D.W. Shin, K. Chen, O. Gheysens, Q. Cao, S.X. Wang, S.S. Gambhir, X. Chen, Nano Lett. **6**, 669 (2006)
46. M.E. Akerman, W.C.W. Chan, P. Laakkonen, S.N. Bhatia, E. Ruoslahti, Proc. Natl. Acad. Sci. USA **99**, 12617 (2002)
47. F. Pinaud, D. King, H.-P. Moore, S. Weiss, J. Am. Chem. Soc. **126**, 6115 (2004)
48. A.R. Clapp, I.L. Medintz, J.M. Mauro, B.R. Fisher, M.G. Bawendi, H. Mattoussi, J. Am. Chem. Soc. **126**, 301 (2004)
49. I.L. Medintz, S.A. Trammell, H. Mattoussi, J.M. Mauro, J. Am. Chem. Soc. **126**, 30 (2004)
50. I.L. Medintz, J.H. Konnert, A.R. Clapp, I. Stanish, M.E. Twigg, H. Mattoussi, J.M. Mauro, J.R. Deschamps, Proc. Natl. Acad. Sci. USA **101**, 9612 (2004)
51. K. Hanaki, A. Momo, T. Oku, A. Komoto, S. Maenosono, Y. Yamaguchi, K. Yamamoto, Biochem. Biophys. Res. Commun. **302**, 496 (2003)
52. E.R. Goldman, G.P. Anderson, P.T. Tran, H. Mattoussi, P.T. Charles, J.M. Mauro, Anal. Chem. **74**, 841 (2002)
53. H. Mattoussi, J. Am. Chem. Soc. **122**, 12142 (2000)

54. H. Mattoussi, J.M. Mauro, E.R. Goldman, T.M. Green, G.P. Anderson, Phys. Status Solidi. B-Basic Res. **224**, 277 (2001)
55. A.P. Alivisatos, W. Gu, C. Larabell, Annu. Rev. Biomed. Eng. **7**, 55 (2005)
56. F. Pinaud, X. Michalet, L.A. Bentolila, J.M. Tsay, S. Doose, J.J. Li, G. Iyer, S. Weiss, Biomaterials **27**, 1679 (2006)
57. A.M. Smith, G. Ruan, M.N. Rhyner, S. Nie, Ann. Biomed. Eng. **34**, 3 (2006)
58. M.P. Bruchez, Curr. Opin. Chem. Biol. **9**, 533 (2005)
59. F. Chen, D. Gerion, Nano Lett. **4**, 1827 (2004)
60. Z. Kaul, T. Yaguchi, S.C. Kaul, T. Hirano, R. Wadhwa, K. Taira, Cell Res. **13**, 503 (2003)
61. A. Mansson, M. Sundberg, M. Balaz, R. Bunk, I.A. Nicholls, P. Omling, S. Tagerud, L. Montelius, Biochem. Biophys. Res. Commun. **314**, 529 (2004)
62. D. Ishii, K. Kinbara, Y. Ishida, N. Ishii, M. Okochi, M. Yohda, T. Aida, Nature **423**, 628 (2003)
63. J.K. Jaiswal, H. Mattoussi, J.M. Mauro, S.M. Simon, Nat. Biotechnol. **21**, 47 (2003)
64. D.S. Lidke, P. Nagy, R. Heintzmann, D.J. Arndt-Jovin, J.N. Post, H.E. Grecco, E.A. Jares-Erijman, T.M. Jovin, Nat. Biotechnol. **22**, 198 (2004)
65. A. Sukhanova, J. Devy, L. Venteo, H. Kaplan, M. Artemyev, V. Oleinikov, D. Klinov, M. Pluot, J.H. Cohen, I. Nabiev, Anal. Biochem. **324**, 60 (2004)
66. F. Tokumasu, J. Dvorak, J. Microsc. **211**, 256 (2003)
67. O. Minet, C. Dressler, J. Beuthan, J. Fluoresc. **14**, 241 (2004)
68. T.D. Lacoste, X. Michalet, F. Pinaud, D.S. Chemla, A.P. Alivisatos, S. Weiss, Proc. Natl. Acad. Sci. USA **97**, 9461 (2000)
69. A.M. Smith, S. Dave, S. Nie, L. True, X. Gao, Expert Rev. Mol. Diagn. **6**, 231 (2006)
70. R.G. Neuhauser, K.T. Shimizu, W.K. Woo, S.A. Empedocles, M.G. Bawendi, Phys. Rev. Lett. **85**, 3301 (2000)
71. J. Yao, D.R. Larson, H.D. Vishwasrao, W.R. Zipfel, W.W. Webb, Proc. Natl. Acad. Sci. USA **102**, 14284 (2005)
72. S. Hohng, T. Ha, J. Am. Chem. Soc. **126**, 1324 (2004)
73. D.R. Larson, W.R. Zipfel, R.M. Williams, S.W. Clark, M.P. Bruchez, F.W. Wise, W.W. Webb, Science **300**, 1434 (2003)
74. T. Pellegrino, W.J. Parak, R. Boudreau, M.A. Le Gros, D. Gerion, A.P. Alivisatos, C.A. Larabell, Differentiation **71**, 542 (2003)
75. L.C. Mattheakis, J.M. Dias, Y.J. Choi, J. Gong, M.P. Bruchez, J. Liu, E. Wang, Anal. Biochem. **327**, 200 (2004)
76. S. Ramachandran, N.E. Merrill, R.H. Blick, D.W. van der Weide, Biosens. Bioelectron. **20**, 2173 (2005)
77. J.A. Kloepfer, R.E. Mielke, M.S. Wong, K.H. Nealson, G. Stucky, J.L. Nadeau, Appl. Environ. Microbiol. **69**, 4205 (2003)
78. F. Osaki, T. Kanamori, S. Sando, T. Sera, Y. Aoyama, J. Am. Chem. Soc. **126**, 6520 (2004)
79. J. Nath, K.L. Johnson, Biotech. Histochem. **73**, 6 (1998)
80. J. Nath, K.L. Johnson, Biotech. Histochem. **75**, 54 (2000)
81. P. Chan, T. Yuen, F. Ruf, J. Gonzalez-Maeso, S.C. Sealfon, Nucleic Acids Res. **33**, e161 (2005)
82. D. Gerion, W.J. Parak, S.C. Williams, D. Zanchet, C.M. Micheel, A.P. Alivisatos, J. Am. Chem. Soc. **124**, 7070 (2002)
83. J.R. Lakowicz, I. Gryczynski, Z. Gryczynski, K. Nowaczyk, C.J. Murphy, Anal. Biochem. **280**, 128 (2000)
84. R. Mahtab, H.H. Harden, C.J. Murphy, J. Am. Chem. Soc. **122**, 14 (2000)
85. G.P. Mitchell, C.A. Mirkin, R.L. Letsinger, J. Am. Chem. Soc. **121**, 8122 (1999)
86. W.J. Parak, R. Boudreau, M. Le Gros, D. Gerion, D. Zanchet, C.M. Micheel, S.C. Williams, A.P. Alivisatos, C. Larabell, Adv. Mater. **14**, 882 (2002)
87. S. Pathak, S.K. Choi, N. Arnheim, M.E. Thompson, J Am Chem Soc **123**, 4103 (2001)
88. Y. Xiao, P.E. Barker, Nucleic Acids Res. **32**, e28 (2004)
89. Y. Xiao, W.G. Telford, J.C. Ball, L.E. Locascio, P.E. Barker, Nat. Methods **2**, 723 (2005)
90. S.M. Wu, X. Zhao, Z.L. Zhang, H.Y. Xie, Z.Q. Tian, J. Peng, Z.X. Lu, D.W. Pang, Z.X. Xie, Chemphyschem **7**, 1062 (2006)
91. L. Stryer, Annu. Rev. Biochem. **47**, 819 (1978)
92. E.A. Jares-Erijman, T.M. Jovin, Nat. Biotechnol. **21**, 1387 (2003)
93. E.A. Jares-Erijman, T.M. Jovin, Curr. Opin. Chem. Biol. **10**, 409 (2006)
94. C.R. Kagan, C.B. Murray, M.G. Bawendi, Phys. Rev. B **54**, 8633 (1996)
95. C.R. Kagan, C.B. Murray, M. Nirmal, M.G. Bawendi, Phys. Rev. Lett. **76**, 1517 (1996)
96. I.L. Medintz, A.R. Clapp, H. Mattoussi, E.R. Goldman, B. Fisher, J.M. Mauro, Nat. Mater. **2**, 630 (2003)
97. Y. Nagasaki, T. Ishii, Y. Sunaga, Y. Watanabe, H. Otsuka, K. Kataoka, Langmuir **20**, 6396 (2004)
98. E. Oh, M.Y. Hong, D. Lee, S.H. Nam, H.C. Yoon, H.S. Kim, J. Am. Chem. Soc. **127**, 3270 (2005)
99. F. Patolsky, R. Gill, Y. Weizmann, T. Mokari, U. Banin, I. Willner, J. Am. Chem. Soc. **125**, 13918 (2003)
100. D.M. Willard, L.L. Carillo, J. Jung, A. van Orden, Nano Lett. **1**, 469 (2001)
101. A.R. Clapp, I.L. Medintz, H. Mattoussi, Chemphyschem **7**, 47 (2006)
102. I.L. Medintz, A.R. Clapp, F.M. Brunel, T. Tiefenbrunn, H. Tetsuo Uyeda, E.L. Chang, J.R. Deschamps, P.E. Dawson, H. Mattoussi, Nat. Mater. **5**, 581 (2006)
103. S. Hohng, T. Ha, Chemphyschem **6**, 956 (2005)
104. A.R. Clapp, I.L. Medintz, B.R. Fisher, G.P. Anderson, H. Mattoussi, J. Am. Chem. Soc. **127**, 1242 (2005)
105. H.Y. Liu, T.Q. Vu, Nano Lett. **7**, 1044 (2007)
106. R. Bakalova, Z. Zhelev, H. Ohba, Y. Baba, J. Am. Chem. Soc. **127**, 9328 (2005)
107. R.L. Ornberg, T.F. Harper, H. Liu, Nat. Methods **2**, 79 (2005)
108. S.C. Makrides, C. Gasbarro, J.M. Bello, Biotechniques **39**, 501 (2005)
109. B.N. Giepmans, T.J. Deerinck, B.L. Smarr, Y.Z. Jones, M.H. Ellisman, Nat. Methods **2**, 743 (2005)
110. R. Nisman, G. Dellaire, Y. Ren, R. Li, D.P. Bazett-Jones, J. Histochem. Cytochem. **52**, 13 (2004)
111. Y. Zhang, M.K. So, J. Rao, Nano Lett. **6**, 1988 (2006)
112. H. Duan, S. Nie, J. Am. Chem. Soc. **129**, 3333 (2007)
113. S. Courty, C. Luccardini, Y. Bellaiche, G. Cappello, M. Dahan, Nano Lett. **6**, 1491 (2006)
114. M. Han, X. Gao, J.Z. Su, S. Nie, Nat. Biotechnol. **19**, 631 (2001)
115. H. Xu, M.Y. Sha, E.Y. Wong, J. Uphoff, Y. Xu, J.A. Treadway, A. Truong, E. O'Brien, S. Asquith, M. Stubbins, N.K. Spurr, E.H. Lai, W. Mahoney, Nucleic Acids Res. **31**, e43 (2003)
116. S.J. Rosenthal, Nat. Biotechnol. **19**, 621 (2001)
117. E. Katz, I. Willner, Angew. Chem. Int. Ed. Engl. **43**, 6042 (2004)
118. A.A. Chen, A.M. Derfus, S.R. Khetani, S.N. Bhatia, Nucleic Acids Res. **33**, e190 (2005)
119. M. Howarth, K. Takao, Y. Hayashi, A.Y. Ting, Proc. Natl. Acad. Sci. USA **102**, 7583 (2005)
120. M. Olek, T. Busgen, M. Hilgendorff, M. Giersig, J. Phys. Chem. B Condens. Matter Mater. Surf. Interfaces Biophys. **110**, 12901 (2006)
121. Y.T. Lim, S. Kim, A. Nakayama, N.E. Stott, M.G. Bawendi, J.V. Frangioni, Mol. Imaging **2**, 50 (2003)
122. J.V. Frangioni, Curr. Opin. Chem. Biol. **7**, 626 (2003)
123. G. Reich, Adv. Drug. Deliv. Rev. **57**, 1109 (2005)
124. C. Bremer, C.H. Tung, R. Weissleder, Nat. Med. **7**, 743 (2001)

125. R. Weissleder, C.H. Tung, U. Mahmood, A. Bogdanov Jr., Nat. Biotechnol. **17**, 375 (1999)
126. A.E. Cerussi, A.J. Berger, F. Bevilacqua, N. Shah, D. Jakubowski, J. Butler, R.F. Holcombe, B.J. Tromberg, Acad. Radiol. **8**, 211 (2001)
127. E.B. Voura, J.K. Jaiswal, H. Mattoussi, S.M. Simon, Nat. Med. **10**, 993 (2004)
128. S. Rieger, R.P. Kulkarni, D. Darcy, S.E. Fraser, R.W. Koster, Dev. Dyn. **234**, 670 (2005)
129. M. Stroh, J.P. Zimmer, D.G. Duda, T.S. Levchenko, K.S. Cohen, E.B. Brown, D.T. Scadden, V.P. Torchilin, M.G. Bawendi, D. Fukumura, R.K. Jain, Nat. Med. **11**, 678 (2005)
130. M.J. Levene, D.A. Dombeck, K.A. Kasischke, R.P. Molloy, W.W. Webb, J. Neurophysiol. **91**, 1908 (2004)
131. N.Y. Morgan, S. English, W. Chen, V. Chernomordik, A. Russo, P.D. Smith, A. Gandjbakhche, Acad. Radiol. **12**, 313 (2005)
132. J.D. Smith, G.W. Fisher, A.S. Waggoner, P.G. Campbell, Microvasc. Res. **73**, 75 (2007)
133. S. Kim, B. Fisher, H.J. Eisler, M. Bawendi, J. Am. Chem. Soc. **125**, 11466 (2003)
134. E.G. Soltesz, S. Kim, R.G. Laurence, A.M. DeGrand, C.P. Parungo, D.M. Dor, L.H. Cohn, M.G. Bawendi, J.V. Frangioni, T. Mihaljevic, Ann. Thorac. Surg. **79**, 269 (2005)
135. C.P. Parungo, S. Ohnishi, S.W. Kim, S. Kim, R.G. Laurence, E.G. Soltesz, F.Y. Chen, Y.L. Colson, L.H. Cohn, M.G. Bawendi, J.V. Frangioni, J. Thorac. Cardiovasc. Surg. **129**, 844 (2005)
136. E.G. Soltesz, S. Kim, S.W. Kim, R.G. Laurence, A.M. De Grand, C.P. Parungo, L.H. Cohn, M.G. Bawendi, J.V. Frangioni, Ann. Surg. Oncol. **13**, 386 (2006)
137. J.P. Zimmer, S.W. Kim, S. Ohnishi, E. Tanaka, J.V. Frangioni, M.G. Bawendi, J. Am. Chem. Soc. **128**, 2526 (2006)
138. S.W. Kim, J.P. Zimmer, S. Ohnishi, J.B. Tracy, J.V. Frangioni, M.G. Bawendi, J. Am. Chem. Soc. **127**, 10526 (2005)
139. C.P. Parungo, Y.L. Colson, S.W. Kim, S. Kim, L.H. Cohn, M.G. Bawendi, J.V. Frangioni, Chest **127**, 1799 (2005)
140. C.P. Parungo, D.I. Soybel, Y.L. Colson, S.W. Kim, S. Ohnishi, A.M. De Grand, R.G. Laurence, E.G. Soltesz, F.Y. Chen, L.H. Cohn, M.G. Bawendi, J.V. Frangioni, Ann. Surg. Oncol. **14**, 286 (2007)
141. J.V. Frangioni, S.W. Kim, S. Ohnishi, S. Kim, M.G. Bawendi, Methods Mol. Biol. **374**, 147 (2007)
142. Y. Hama, Y. Koyama, Y. Urano, P.L. Choyke, H. Kobayashi, Breast Cancer Res. Treat. **103**, 23 (2007)
143. B. Ballou, L.A. Ernst, S. Andreko, T. Harper, J.A. Fitzpatrick, A.S. Waggoner, M.P. Bruchez, Bioconjug. Chem. **18**, 389 (2007)
144. C. Nicholson, J. Neural. Transm. **112**, 29 (2005)
145. C. Nicholson, K.C. Chen, S. Hrabetova, L. Tao, Prog. Brain Res. **125**, 129 (2000)
146. R.G. Thorne, C. Nicholson, Proc. Natl. Acad. Sci. USA **103**, 5567 (2006)
147. O. Muhammad, A. Popescu, S.A. Toms, Methods Mol. Biol. **374**, 161 (2007)
148. M.D. Chavanpatil, A. Khdair, J. Panyam, J. Nanosci. Nanotechnol. **6**, 2651 (2006)
149. M.A. Popescu, S.A. Toms, Expert Rev. Mol. Diagn. **6**, 879 (2006)
150. H. Jackson, O. Muhammad, H. Daneshvar, J. Nelms, A. Popescu, M.A. Vogelbaum, M. Bruchez, S.A. Toms, Neurosurgery **60**, 524 (2007)
151. B. Ballou, B.C. Lagerholm, L.A. Ernst, M.P. Bruchez, A.S. Waggoner, Bioconjug. Chem. **15**, 79 (2004)
152. B. Ballou, Curr. Top. Dev. Biol. **70**, 103 (2005)
153. D. Rajotte, E. Ruoslahti, J. Biol. Chem. **274**, 11593 (1999)
154. D. Rajotte, W. Arap, M. Hagedorn, E. Koivunen, R. Pasqualini, E. Ruoslahti, J. Clin. Invest. **102**, 430 (1998)
155. K. Porkka, P. Laakkonen, J.A. Hoffman, M. Bernasconi, E. Ruoslahti, Proc. Natl. Acad. Sci. USA **99**, 7444 (2002)
156. P. Laakkonen, K. Porkka, J.A. Hoffman, E. Ruoslahti, Nat. Med. **8**, 751 (2002)
157. W. Cai, X. Chen, Anti-Cancer Agents Med. Chem. **6**, 407 (2006)
158. W. Cai, J. Rao, S.S. Gambhir, X. Chen, Mol. Cancer Ther. **5**, 2624 (2006)
159. W. Cai, S.S. Gambhir, X. Chen, Biotechniques **39**, S6 (2005)
160. W. Cai, Y. Wu, K. Chen, Q. Cao, D.A. Tice, X. Chen, Cancer Res. **66**, 9673 (2006)
161. W. Cai, X. Zhang, Y. Wu, X. Chen, J. Nucl. Med. **47**, 1172 (2006)
162. X. Chen, P.S. Conti, R.A. Moats, Cancer Res. **64**, 8009 (2004)
163. Y. Wu, X. Zhang, Z. Xiong, Z. Cheng, D.R. Fisher, S. Liu, X. Chen, J. Nucl. Med. **46**, 1707 (2005)
164. Z. Xiong, Z. Cheng, X. Zhang, M. Patel, J.C. Wu, S.S. Gambhir, X. Chen, J. Nucl. Med. **47**, 130 (2006)
165. X. Zhang, Z. Xiong, X. Wu, W. Cai, J.R. Tseng, S.S. Gambhir, X. Chen, J. Nucl. Med. **47**, 113 (2006)
166. H. Maeda, J. Wu, T. Sawa, Y. Matsumura, K. Hori, J. Control. Release **65**, 271 (2000)
167. T. Tanaka, S. Shiramoto, M. Miyashita, Y. Fujishima, Y. Kaneo, Int. J. Pharm. **277**, 39 (2004)
168. W. Cai, K. Chen, K.A. Mohamedali, Q. Cao, S.S. Gambhir, M.G. Rosenblum, X. Chen, J. Nucl. Med. **47**, 2048 (2006)
169. W. Cai, X. Chen, Front. Biosci. **12**, 4267 (2007)
170. N. Ferrara, Endocr. Rev. **25**, 581 (2004)
171. S.S. Chang, V.E. Reuter, W.D. Heston, P.B. Gaudin, Urology **57**, 801 (2001)
172. R.M. Levenson, Lab. Med. **35**, 244 (2004)
173. J.R. Mansfield, K.W. Gossage, C.C. Hoyt, R.M. Levenson, J. Biomed. Opt. **10**, 41207 (2005)
174. X. Yu, L. Chen, K. Li, Y. Li, S. Xiao, X. Luo, J. Liu, L. Zhou, Y. Deng, D. Pang, Q. Wang, J. Biomed. Opt. **12**, 014008 (2007)
175. H. Tada, H. Higuchi, T.M. Wanatabe, N. Ohuchi, Cancer Res. **67**, 1138 (2007)
176. M.K. So, C. Xu, A.M. Loening, S.S. Gambhir, J. Rao, Nat. Biotechnol. **24**, 339 (2006)
177. C.H. Contag, M.H. Bachmann, Annu. Rev. Biomed. Eng. **4**, 235 (2002)
178. R.S. Negrin, C.H. Contag, Nat. Rev. Immunol. **6**, 484 (2006)
179. A.M. Loening, T.D. Fenn, A.M. Wu, S.S. Gambhir, Protein Eng. Des. Sel. **19**, 391 (2006)
180. Y. Zhang, M.K. So, A.M. Loening, H. Yao, S.S. Gambhir, J. Rao, Angew. Chem. Int. Ed. Engl. **45**, 4936 (2006)
181. V.L. Colvin, Nat. Biotechnol. **21**, 1166 (2003)
182. P.H. Hoet, I. Bruske-Hohlfeld, O.V. Salata, J. Nanobiotechnology **2**, 12 (2004)
183. R. Hardman, Environ. Health Perspect. **114**, 165 (2006)
184. J.M. Tsay, X. Michalet, Chem. Biol. **12**, 1159 (2005)
185. A.M. Derfus, W.C.W. Chan, S.N. Bhatia, Nano Lett. **4**, 11 (2004)
186. R. Nath, R. Prasad, V.K. Palinal, R.K. Chopra, Prog. Food Nutr. Sci. **8**, 109 (1984)
187. C. Kirchner, T. Liedl, S. Kudera, T. Pellegrino, A.M. Javier, H.E. Gaub, S. Stoelzle, N. Fertig, W.J. Parak, Nano Lett. **5**, 331 (2005)
188. R. Bakalova, H. Ohba, Z. Zhelev, M. Ishikawa, Y. Baba, Nat. Biotechnol. **22**, 1360 (2004)
189. A.C. Samia, X. Chen, C. Burda, J. Am. Chem. Soc. **125**, 15736 (2003)
190. L. Landin, M.S. Miller, M. Pistol, C.E. Pryor, L. Samuelson, Science **280**, 262 (1998)

191. N. Tanaka, J. Yamasaki, S. Fuchi, Y. Takeda, Microsc. Microanal. **10**, 139 (2004)
192. N. Pradhan, D. Goorskey, J. Thessing, X. Peng, J. Am. Chem. Soc. **127**, 17586 (2005)
193. N. Pradhan, D.M. Battaglia, Y. Liu, X. Peng, Nano Lett. **7**, 312 (2007)
194. W. Guo, J.J. Li, Y.A. Wang, X. Peng, J. Am. Chem. Soc. **125**, 3901 (2003)
195. Y. Liu, M. Kim, Y. Wang, Y.A. Wang, X. Peng, Langmuir **22**, 6341 (2006)
196. T.F. Massoud, S.S. Gambhir, Genes Dev. **17**, 545 (2003)
197. X. Montet, V. Ntziachristos, J. Grimm, R. Weissleder, Cancer Res. **65**, 6330 (2005)
198. X. Montet, J.L. Figueiredo, H. Alencar, V. Ntziachristos, U. Mahmood, R. Weissleder, Radiology **242**, 751 (2007)
199. V. Ntziachristos, C.H. Tung, C. Bremer, R. Weissleder, Nat. Med. **8**, 757 (2002)
200. S. Wang, B.R. Jarrett, S.M. Kauzlarich, A.Y. Louie, J. Am. Chem. Soc. **129**, 3848 (2007)
201. S.T. Selvan, P.K. Patra, C.Y. Ang, J.Y. Ying, Angew. Chem. Int. Ed. Engl. **46**, 2448 (2007)
202. W.J. Mulder, R. Koole, R.J. Brandwijk, G. Storm, P.T. Chin, G.J. Strijkers, C. de Mello Donega, K. Nicolay, A.W. Griffioen, Nano Lett. **6**, 1 (2006)
203. G.A. van Tilborg, W.J. Mulder, P.T. Chin, G. Storm, C.P. Reutelingsperger, K. Nicolay, G.J. Strijkers, Bioconjug. Chem. **17**, 865 (2006)
204. L. Prinzen, R.J. Miserus, A. Dirksen, T.M. Hackeng, N. Deckers, N.J. Bitsch, R.T. Megens, K. Douma, J.W. Heemskerk, M.E. Kooi, P.M. Frederik, D.W. Slaaf, M.A. van Zandvoort, C.P. Reutelingsperger, Nano Lett. **7**, 93 (2007)
205. D. Wang, J. He, N. Rosensweig, Z. Rosenzweig, Nano Lett. **4**, 409 (2004)
206. H. Gu, R. Zheng, X. Zhang, B. Xu, J. Am. Chem. Soc. **126**, 5664 (2004)
207. W. Cai, K. Chen, Z.B. Li, S.S. Gambhir, X. Chen, J. Nucl. Med. submitted (2007)
208. W. Cai, K. Chen, L. He, Q. Cao, A. Koong, X. Chen, Eur. J. Nucl. Med. Mol. Imaging Epub (2007)
209. A.R. Hsu, W. Cai, A. Veeravagu, K.A. Mohamedali, K. Chen, S. Kim, H. Vogel, L.C. Hou, V. Tse, M.G. Rosenblum, X. Chen, J. Nucl. Med. **48**, 445 (2007)
210. P. Taroni, G. Danesini, A. Torricelli, A. Pifferi, L. Spinelli, R. Cubeddu, J. Biomed. Opt. **9**, 464 (2004)
211. X. Intes, Acad. Radiol. **12**, 934 (2005)